

Supplementary material

Deciphering and predicting spatial and temporal concentrations of arsenic within the Mekong Delta aquifer

Benjamin Kocar^A, *Shawn Benner*^B and *Scott Fendorf*^{C,D}

^AParsons Laboratory, Department of Civil and Environmental Engineering, Massachusetts Institute of Technology, Cambridge, MA 02139, USA.

^BDepartment of Geosciences, 1910 University Drive, Boise State University, Boise, ID 83725, USA.

^CDepartment of Environmental & Earth System Science, Stanford University, Stanford, CA 94305, USA.

^DCorresponding author. Email: Fendorf@stanford.edu

Aqueous sampling and analysis

A peristaltic pump (Geopump II, Geotech Environmental Equipment, Inc.) was used to draw well water at a rate of $\sim 1 \text{ L min}^{-1}$ into a flow cell (YSI Inc., Ohio, USA) housing a YSI 556 multiparameter probe. Temperature, Eh, pH, conductivity, and dissolved oxygen (DO) were continuously measured and recorded upon stabilisation, which typically occurred within ~ 10 min. Upon DO stabilisation, groundwater samples were filtered into acid washed bottles. Samples taken for cation and arsenic measurement were acidified with trace metal grade HCl, while samples taken for sulfate analysis were pretreated with Bio-Rad AG50W-X8 cation exchange resin to eliminate metals from solution, which could precipitate and scavenge anions. Lysimeters (Prenart Equipment ApS) were allowed to equilibrate with porewater for 30 days; during this time, several samples were collected and discarded, and sampling commenced from 2006 to 2007. Porewater was drawn by suction (-800 mBar) into bottles, each containing 15 mL of TraceMetal grade 3 M HCl. Surface water was collected on a monthly basis at the water-air interface. Sample collection was identical to the groundwater samples.

Arsenic was measured in the laboratory with hydride generation inductively coupled plasma atomic emission spectroscopy (HG-ICP-AES). Briefly, 1 mL of 5% KI in 12M HCl was added to 3 mL of sample to pre-reduce As(V) to As(III). Arsine gas was generated by addition of 0.5% NaBH₄/0.5% NaOH and quantified with HG-ICP-AES^[1]; the detection limit using this method was $5 \mu\text{g L}^{-1}$. Sample Ca and Fe were measured by ICP-AES, and quality control standards were monitored throughout the course of the analysis. Sulfate was analysed with a Dionex 500DX ion chromatograph using an AS9 guard/high capacity column, with a flow rate of 1.0 mL min^{-1} and using a 9 mM Na₂CO₃ isocratic eluent. Field measurements on aqueous samples were performed to quantify alkalinity and NH₄⁺. Alkalinity was determined by titrating samples with 1.6 M H₂SO₄ to a colourimetric endpoint using a Hach digital titrator

and bromocrescol green-methyl red indicator (Hach). NH_4^+ was measured with a Hach DR 2400 portable spectrophotometer using defined protocols.

Solid phase collection and analysis

A set of intact core samples were collected with an AMS soil coring device, anaerobically preserved with gas-tight plastic bags and Mitsubishi Anaerobic packs, and dried and homogenised in a Coy anaerobic glovebag. Samples were then passed through a 200- μm sieve to remove woody and miscellaneous debris. Three approaches were used to characterise iron solids collected between 0 and 4 m of our field site: selective extractions, XAS analysis (including Extended X-ray Absorption Structure – EXAFS – and X-ray Absorption Near Edge Structure – XANES – spectroscopies) and conventional or synchrotron X-ray diffraction (sXRD). Owing to the limited quantity of intact material, samples taken from 7- and 14-m cores were only subjected to chemical extractions.

Sediments were subjected to chemical extraction to target weakly bound (DI water), salt displaceable (1 M MgCl_2), ligand displaceable (1 M PO_4^{3-} , pH 5.0), acid digestible (1 M HCl nominally for AVS/carbonates/amorphous oxides), and reducible metal (Fe and Mn) oxides (citrate-bicarbonate-dithionate extraction).^[2] Total digestions were also performed on 0.1 g of sample following USA EPA protocol 3052 (3 : 1 concentrated HNO_3 :concentrated HF). The digested sediments were then evaporated and reconstituted in HCl. All extracts and digests were measured by ICP-AES or HG-ICP-AES (for arsenic) as described above.

Conventional and synchrotron X-ray diffraction were used for identification of minerals and silicate clays which may harbor iron **and/or** arsenic within sediments. Ground samples from 1 and 4 m at site T were anaerobically sealed within 2 layers of Kapton tape, and synchrotron-XRD was performed at 12 735 eV on beamline 11–3 at SSRL which was equipped with a Si(311) monochromator and a MAR345 imaging plate. Diffraction patterns were analysed with JADE 6.0 (Materials Data, Inc.). To identify clay minerals, aliquots of sediment were first pre-treated with citrate-bicarbonate-dithionate to remove iron and manganese (hydr)oxides. After centrifugation, the remaining clay fraction was treated with MgCl_2 /air-drying, MgCl_2 /glycerol, KCl/air-drying or KCl/500 °C-heating to differentiate different clay minerals. Conventional XRD analysis (Cu $K\alpha$ radiation) was used to confirm the dominant clay fractions associated with each treatment.

Iron EXAFS spectra of anaerobically preserved sediments were collected at beamline 11–2 at the Stanford Synchrotron Radiation Lightsource (SSRL). Incident and transmission intensities were measured using in-line ionization chambers and sample fluorescence via a wide-angle ionization chamber equipped with Soller slits and Mn filters. A double crystal Si(220) monochromator was used for energy selection.

Scans were conducted from 100 eV below to 1000 eV above the Fe K-edge at 7111 eV. Data analysis and interpretation was performed through linear combination fits of iron standard spectra constrained by solid phase extraction data and solids identified with XRD/sXRD. Given the appreciable quantity of easily extractable iron within some sediment samples, we included 6-line ferrihydrite and siderite in our fitting routines. Additionally, sXRD proved the existence of hematite, and also provided evidence for siderite. Since smectitic clay was identified in our samples with conventional XRD, ferruginous smectite was also included in our analysis. Amphibole (hornblende) was used as a proxy for recalcitrant iron in our samples, since reducible (CBD extractable) was not equivalent to total iron. Finally, goethite was also included within our fits, as it is often found in close association with hematite, sediment samples often possessed a characteristic yellow hue, and since the addition of goethite often substantially improved the goodness of fit parameter (reduced Chi-square). Most unknown samples were well described with the spectra of 3–4 known materials, whereas three samples (0–0.1 m and flood-borne sediments) were best described with 5 known components (Table 2EA). After fitting, the fraction of components representing minerals targeted by 1 M HCl (6-line ferrihydrite and siderite), CBD (6-line ferrihydrite, siderite, goethite, hematite, and ferruginous smectite), and total iron minus the CBD extraction (amphibole-hornblende) were summed and compared with actual chemical extraction data (Tables 3EA and 4EA). With the exception of sediments collected at 1.0 m, the 1 M HCl, CBD, and total iron fractions estimated from the iron EXAFS fitting closely match the extraction data within ~10% (the approximate error of linear combination fitting).

Arsenic XANES spectra were also collected on beamline 11–2 at SSRL. Incident and transmitted intensity were measured using ion chambers, while X-ray fluorescence was measured using a 13 element Ge detector. Spectra were collected from –150 to 867 eV relative to the As K edge of 11867 eV, and energy calibration was achieved via scanning dilute Na₃AsO₄ after every third sample and setting the first derivative inflection point to 11874 eV. Arsenic XANES spectra were used to examine arsenic speciation.

Influence of seasonally variable flow direction – 2-D simulations

In the base case simulation, the flow field was simplified by neglecting the influence of seasonal shifts in flow direction. This influence was also examined by performing a transient flow simulation with fluctuating river-wetland hydraulic heads and periodic hydraulic gradient reversals. This was achieved by updating simulations with wetland and river stage data collected over a year (Fig. S5), and repeating these sinusoidal patterns for a period of 2500 years. Not unsurprisingly, this transient flow field produces noticeable dispersion (or mixing) of the elevated arsenic plume (Fig. S6, compare panels A and B). Perhaps most noteworthy is elevated arsenic transported in the direction that is net annually up-gradient. However, the overall trend in arsenic concentration at the aquifer scale remains largely unchanged as a

result of periodic gradient reversals, suggesting this aspect of flow complexity has only a modest influence on arsenic behaviour.

Sedimentary organic carbon and iron oxide depletion calculations

Sedimentary particulate organic carbon depletion is determined by making the following calculation: given a soil bulk density of 1.5 g/cc and porosity = 0.5, 1 L of groundwater contacts 1.5 kg of sediment. The median organic carbon content in sediments within our site is 0.37%, which equals 5.55 g C in 1.5 kg of sediment. There is thus 5.55 g (0.46 moles) of C in contact with 1 L of groundwater. Given a depletion rate of 0.13 mmol year⁻¹ L⁻¹ contacting groundwater, organic carbon will be depleted in 3615 years. Similarly, sedimentary iron oxide depletion is found by applying the following calculation. Given a sedimentary CBD-reducible iron (oxide) content of 2%, there are 30 g (0.34 moles as FeOOH) of iron oxide in contact with 1 L of groundwater. Given a simulated iron oxide depletion rate of 0.47 mmol L⁻¹ year⁻¹, iron oxides will be depleted in 714 years.

Table S1. Aqueous chemistry from deep-wetland lysimeters and wells

See Fig. 1, main text for location of intense wetland sampling area

Depth below ground (m)	Arsenic ($\mu\text{g L}^{-1}$)		Iron (mg L^{-1})		Calcium (mg L^{-1})		Sulfate (mg L^{-1})		Ammonia (mg L^{-1})		Bicarbonate (mg L^{-1})				
	<i>n</i>	Average	s.e.	Average	s.e.	Average	s.e.	Average	s.e.	<i>n</i>	Average	s.e.	<i>n</i>	Average	s.e.
Lysimeters															
0.1	25	10.0	3.60	5.43	10.71	57.1	18.9	99.2	15.2	3	0.41	–	2	367	–
0.5	35	27.8	8.30	3.23	5.24	52.3	12.7	33.4	8.6	4	1.72	–	2	461	–
1.0	33	38.6	9.70	5.89	10.36	67.5	15.1	17.2	4.0	6	0.11	–	3	312	–
2.0	36	59.9	12.1	1.34	1.78	45.7	13.1	9.14	1.2	6	0.45	–	2	549	–
4.0	35	88.5	11.4	2.58	3.29	34.5	7.50	8.1	3.3	6	2.43	–	2	740	–
Wells															
1.5	46	22.7	7.10	0.24	0.36	27.5	5.61	40.2	5.4	24	2.71	0.92	16	199	34.9
3.0	53	36.2	5.30	0.19	0.35	38.0	5.27	14.5	2.7	17	13.8	5.37	17	397	77.9
7.0	31	215.0	39.0	1.34	2.35	38.3	6.44	10.5	2.8	9	24.6	14.2	11	527	77.4

Table S2. Dominant iron mineralogy (mol fraction) of Cambodian sediments determined with Fe EXAFS linear combination analysis

Sample depth (m)	6-line Ferrihydrite	Goethite	Hematite	Siderite	Ferruginous smectite	Hornblende	Reduced χ^2
Mekong	0.36	0.10	0.15		0.10	0.28	0.082
Bassac	0.33	0.12	0.14		0.14	0.27	0.126
0.1	0.23	0.08	0.19		0.21	0.29	0.092
0.5		0.30	0.21		0.18	0.31	0.160
1.0		0.18	0.20		0.34	0.28	0.157
2.0			0.19	0.39		0.42	0.155
3.0			0.24	0.38		0.39	0.247
4.0			0.21	0.35		0.44	0.180

Table S3. Iron measured from chemical extractions (Site T)

Depth (m)	Total iron (g kg ⁻¹)	Total – CBD (Recalcitrant Fe) (g kg ⁻¹)	CBD (g kg ⁻¹)	1 M HCl (g kg ⁻¹)
0.1	35.0	9.7	25.3	4.9
0.5	34.1	14.0	20.1	1.7
1.0	43.0	20.1	22.9	2.2
2.0	34.0	12.8	21.2	11.1
3.0	27.9	8.6	19.3	6.2
4.0	33.0	15.0	18.0	8.3

Table S4. Fractions of Fe associated with chemical extractions and inferred from results of Fe EXAFS analysis

All values represent the fraction of total Fe found within a sample (chemical extractions) or the mol % Fe within a sample (Fe EXAFS). Amphibole (hornblende) contribution from Recalcitrant Fe EXAFS analysis. Sum of components used in Reducible Fe EXAFS fitting susceptible to CBD extraction, including 6-line ferrihydrite, goethite, hematite, ferruginous smectite, and siderite. Sum of components used in Easily Extracted EXAFS fitting susceptible to 1 M HCl extraction, including 6-line ferrihydrite and siderite

Depth (m)	Recalcitrant Fe		Reducible Fe		Easily Extracted Fe	
	Total minus CBD Fe (Hornblende)	EXAFS	Chemical Extraction	EXAFSc	Chemical Extraction	EXAFS
0.1	0.28	0.29	0.72	0.71	0.14	0.23
0.5	0.41	0.31	0.59	0.69	0.05	
1.0	0.47	0.28	0.53	0.72	0.05	
2.0	0.38	0.42	0.62	0.58	0.32	0.39
3.0	0.31	0.39	0.69	0.62	0.22	0.38
4.0	0.45	0.44	0.55	0.56	0.25	0.35

Table S5. Position (Å) of Dominant XRD Peaks in Treated Clay Fractions

Cu K α radiation. Sample from 4 m, Site T

Mg saturated, air-dried	Mg saturated, glycerol treatment	K saturated, air-dried	K saturated, heated 500 °C	Minerals
14	14 18	14	13.7, broad	Chlorite Hydroxy-interlayer Smectite
10	10	10	10	Mica
7	7	7	0	Kaolin
3.35				Quartz

Table S6. Simulated relevant components of infiltrating surface waters, based on observed concentrations

Charge balance on chlorine

Parameter	Concentration (mM) unless otherwise stated
O _{2(aq)}	0.21 (partial pressure)
As (umol L ⁻¹)	0.00
CO ₃ ²⁻	5.00
SO ₄ ²⁻	1.00
Cl ⁻	0.16
SiO ₄ ⁴⁻	0.58
Mg ²⁺	0.36
Na ⁺	0.87
Ca ²⁺	0.60
K ⁺	0.60
Mg ²⁺	0.36
Na ⁺	0.87

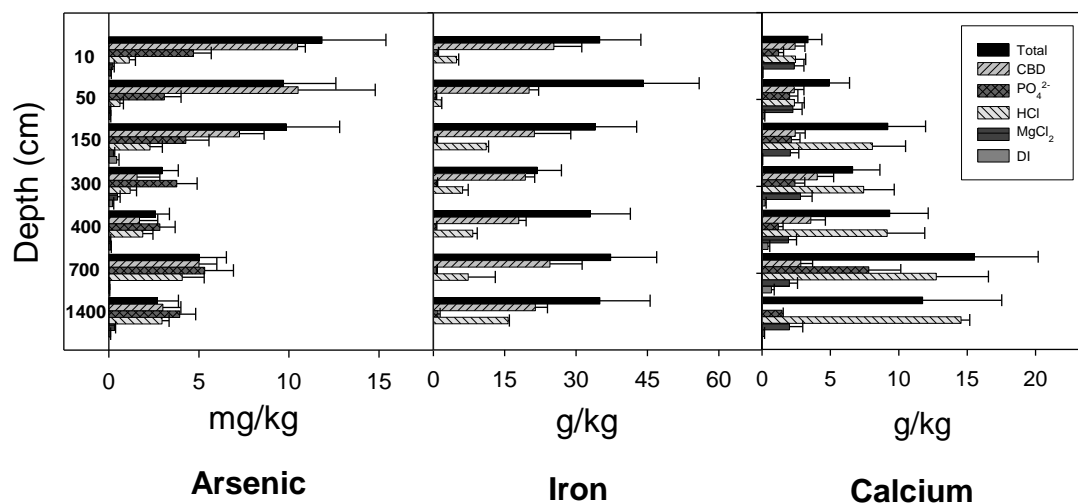


Fig. S1. Selective extractions of wetland sediments as a function of depth. Error bars represent analytical uncertainty.

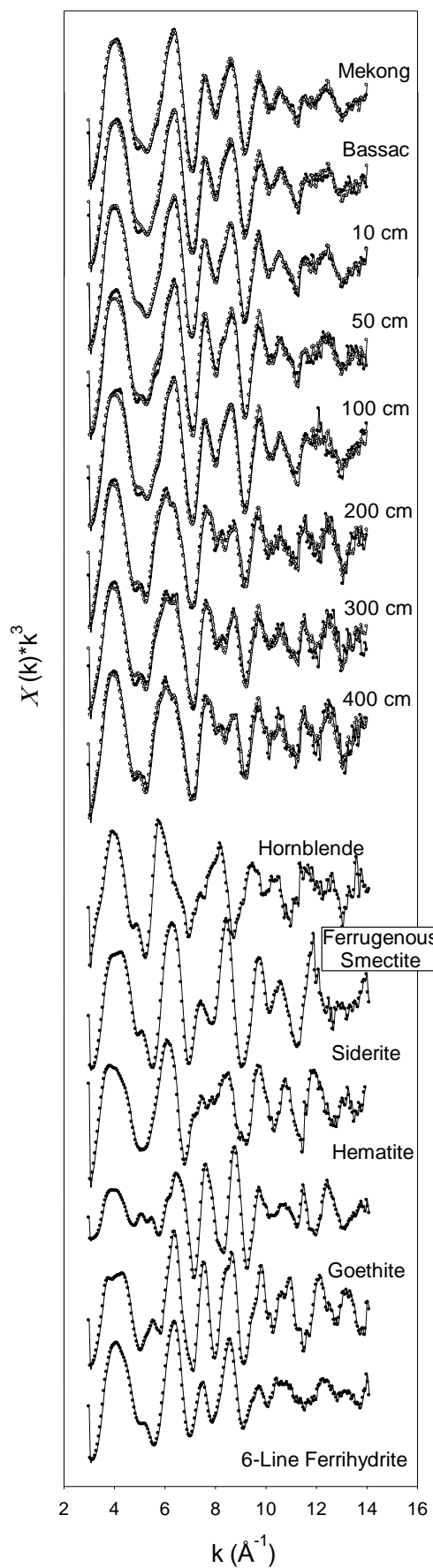


Fig. S2. Least-squares fits (dotted lines) to experimental k^3 weighted Fe-EXAFS spectra (solid lines) obtained for incoming flood-borne sediments (Mekong and Bassac) and for sediments within a 0–4-m profile.

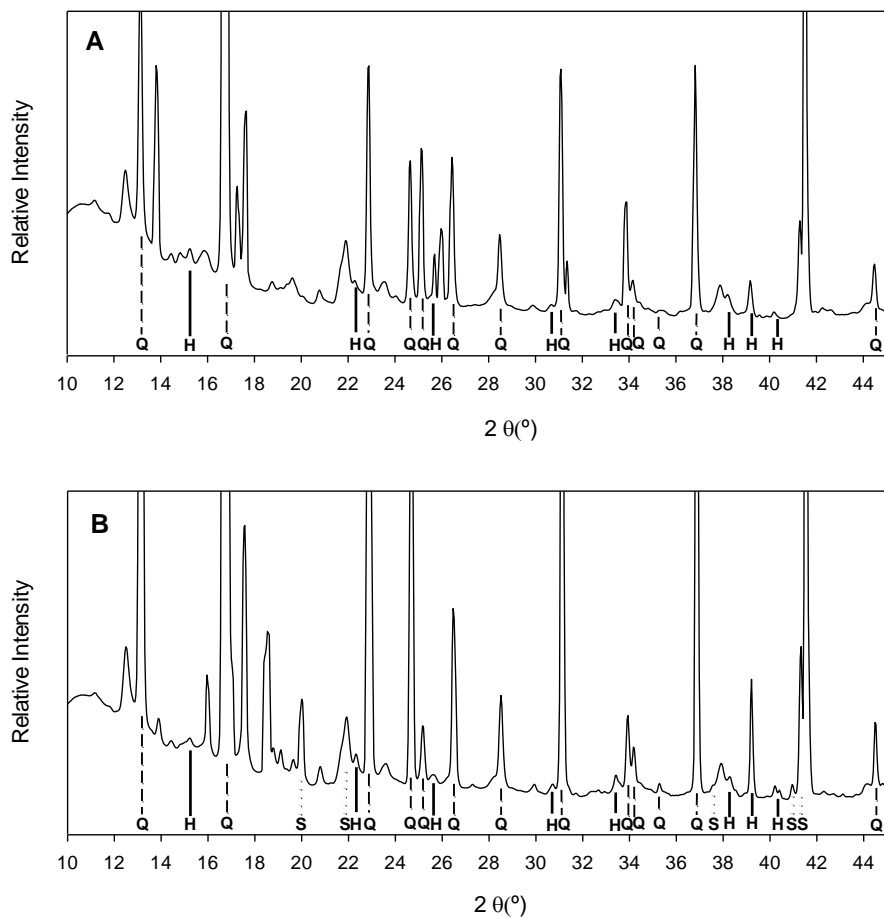


Fig. S3. Synchrotron-XRD patterns of sediments collected at 1 m (A) and 4 m (B). Reflections are labelled for quartz (Q), hematite (H) and siderite (S). Patterns were collected at 12 735 eV.

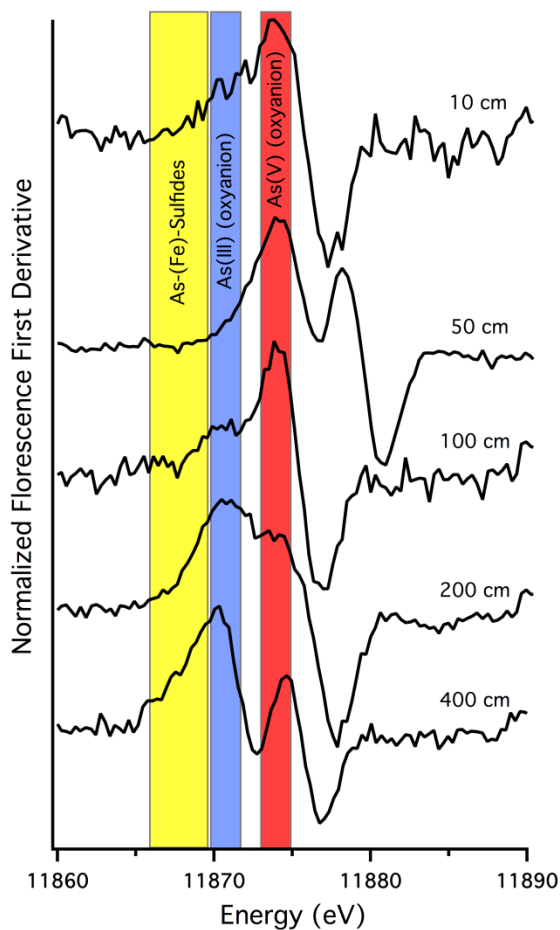


Fig. S4. Arsenic first-derivative XANES collected on intact core samples. Solid(s)-associated arsenic is increasingly reduced as a function of depth, with As^{III} and As^{III} -pyrite representing the dominant species below ~100-cm depth. The apparent As^{V} peak at 400 cm is representative of the first post-edge oscillation in the raw XANES spectra, not the white-line position of As^{V} .

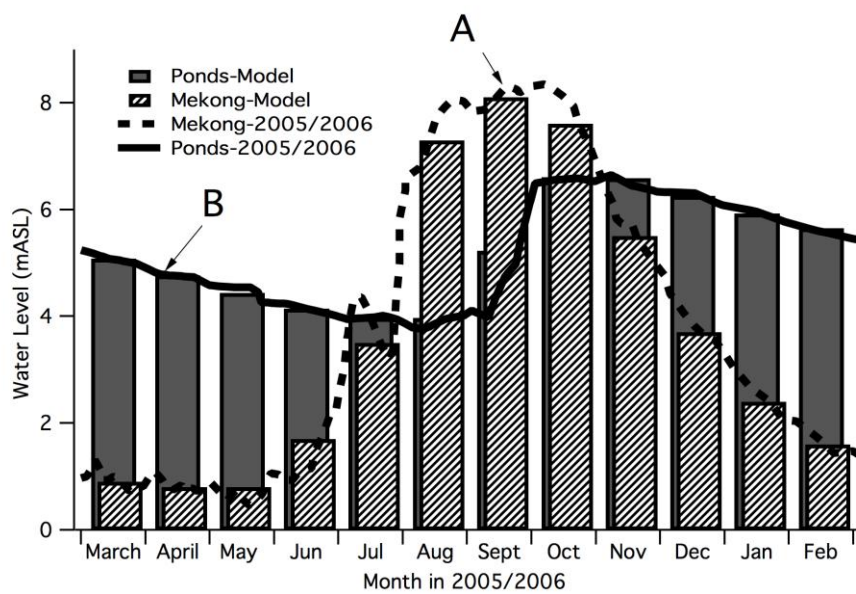


Fig. S5. Mekong River and surface water body hydrographs for 2005–2006. (A, B) represent times where the hydraulic gradient extends from the Mekong towards interior wetlands or from the wetlands to the Mekong, respectively.

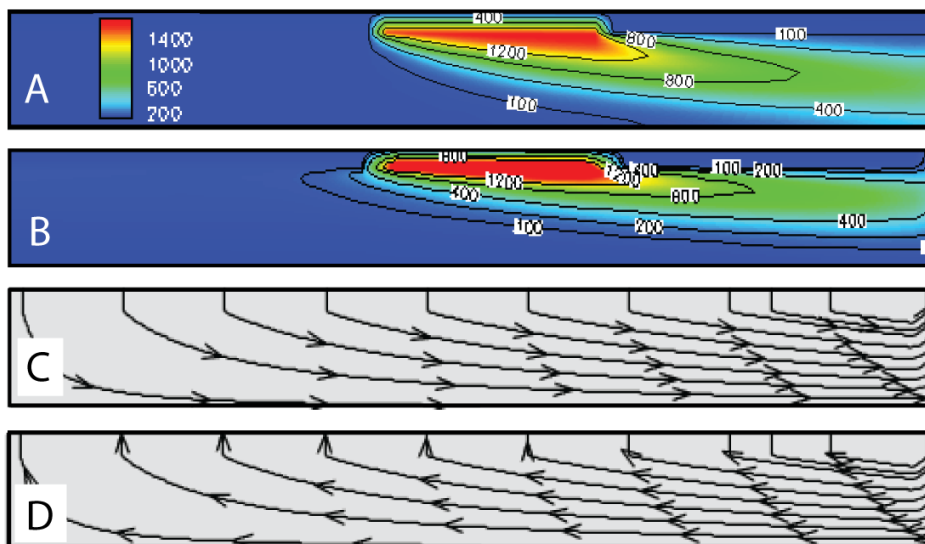


Fig. S6. Transient 2-D simulation. Biogeochemical conditions used in the transient simulation (B) were identical to the base case scenario (A); transient hydrogeologic conditions were supplied using hydrograph data (See Fig. S5) from river and inland surface water bodies, resulting in yearly hydrologic gradient reversals (C, D). Transient hydrologic data was updated monthly, resulting in annually repeating sinusoidal hydrographs, with the annual net direction of groundwater flow extending from the wetlands (oxbows) to the Mekong River. Transient flow field produced discernible dispersion as evidenced by the bulge in elevated arsenic concentrations on the up-gradient side of the plume, and a slight decline (on the order of 10%) in plume arsenic concentrations.

Arsenic sorption to aquifer solids

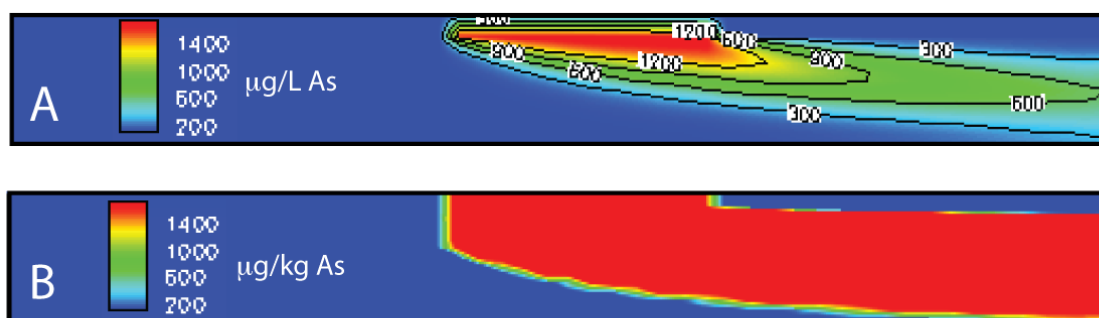


Fig. S7. Simulated arsenic adsorption to aquifer solids. (A) aqueous arsenic concentrations and associated adsorbed arsenic (B) using parameters listed in Table 5 (main text).

References

- [1] P. H. Masscheleyn, R. D. Delaune, W. H. Patrick, A hydride generation atomic-absorption technique for arsenic speciation. *J. Environ. Qual.* **1991**, *20*, 96–100. [doi:10.2134/jeq1991.00472425002000010015x](https://doi.org/10.2134/jeq1991.00472425002000010015x)
- [2] R. H. Loeppert, W. P. Inskeep, [in](#) *Methods of Soil Analysis* (Ed. J. M. Bigham) **1996**, pp. 639–664 (Soil Science Society of America, Inc.: Madison, WI).

Q1 – Please clarify ‘and/or’ – do you mean ‘and’ or ‘or’? The term ‘and/or’ can be seen to be tautologous; ‘or’ (without ‘either’) can logically and grammatically encompass the same meaning as ‘and’ (i.e. ‘or’ does not imply exclusivity between options without ‘either’), and the forward slash logically implies an exclusive ‘or’ in the term (making it somewhat redundantly ‘and [or] or’).

Q2 – cm³?

Q3 – Please provide the chapter or article title you are referring to here.